

Platinum(II) O,O'-Diisobutyl Dithiophosphate: Synthesis, Structure, Thermal Properties, and Solid-State ^{13}C , ^{31}P , and ^{195}Pt CP/MAS NMR Spectra. Model of the Structural State of Platinum in Cooperite

T. A. Rodina^a, I. A. Lutsenko^b, A. V. Gerasimenko^c, and A. V. Ivanov^{b*}

^aAmur State University, Blagoveshchensk, 675027 Russia

^bInstitute of Geology and Nature Management, Amur Scientific Center, Far East Division, Russian Academy of Sciences, Blagoveshchensk, 675000 Russia

^cInstitute of Chemistry, Far East Division, Russian Academy of Sciences, pr. Stoletiya Vladivostoka 159, Vladivostok, 690022 Russia

*E-mail: alexander.v.ivanov@chemist.com

Received November 10, 2008

Abstract—The complex bis(O,O'-diisobutyl dithiophosphato)platinum(II) (**I**) was obtained and characterized by solid-state ^{13}C , ^{31}P , and ^{195}Pt CP/MAS NMR spectroscopy. In complex **I**, the dithiophosphate fragments are structurally equivalent with a predominantly orthorhombic tensor of the ^{31}P chemical shift ($\eta = 0.73$). The tensor of the ^{195}Pt chemical shift approximates to an axially symmetric one (for $\delta_{zz} > \delta_{xx}$ and δ_{yy}), which suggests the existence of square chromophores $[\text{PtS}_4]$, as in cooperite (natural PtS). The crystal and molecular structures of complex **I** were determined from X-ray diffraction data. The Pt atom coordinates two Dtp ligands in a S,S'-anisobidentate fashion (the Pt–S bonds are nonequivalent: 2.315 and 2.329 Å) to form two four-membered chelate rings $[\text{PtS}_2\text{P}]$ with platinum as a spiro atom. The P–S bond length (1.997 and 1.986 Å), which is intermediate between the idealized lengths of the single and double phosphorus–sulfur bonds, suggests the delocalization of the π -electron density in the structural fragments PS_2 . In complex **I**, the electron shielding of the platinum nucleus in the direction perpendicular to the plane of the chromophore $[\text{PtS}_4]$ was found to be noticeably higher than that in cooperite. The thermal properties of complex **I** were examined by combined DSC-TG thermal analysis. The intermediate product of the thermolysis of complex **I** was platinum(II) dithiometaphosphate $[\text{Pt}(\text{S}_2\text{PO})_2]$ and the final thermolysis product was PtS.

DOI: 10.1134/S1070328409070112

The possibility of employing ^{195}Pt (both static and MAS) NMR spectroscopy for the study of natural minerals of platinum has been demonstrated with single-crystal cooperite as an example (natural PtS characterized by R.A. Cooper in 1928) [1, 2]. In cooperite, platinum(II) occupies a central place in the square chromophores $[\text{PtS}_4]$. A structurally similar pattern has been found in platinum(II) complexes with ionic O,O'-dialkyl dithiophosphates (Dtp) [3, 5], which are used as selective collecting agents in the flotation of non-ferrous metal sulfide ores. Gianini et al. have found that the final thermolysis product of these dithiophosphate complexes is PtS as well [4].

Most of the hitherto characterized platinum(II) O,O'-dialkyl dithiophosphates are liquids [4]. That is why the synthesis and study of new crystalline complexes is of interest for the determination of the geometry of the chromophores $[\text{PtS}_4]$ and the character of the anisotropy of the ^{195}Pt and ^{31}P chemical shifts.

In this study, we obtained a new representative of crystalline Pt(II) complexes with Dtp, namely, bis(O,O'-diisobutyl dithiophosphato-S,S')platinum(II) ($[\text{Pt}(\text{S}_2\text{P}(\text{O}-\text{iso}-\text{C}_4\text{H}_9)_2)_2]$ (**I**)) and studied its structure and spectroscopic and thermal properties by X-ray diffraction analysis, ^{13}C , ^{31}P , and ^{195}Pt CP/MAS NMR spectroscopy, and combined thermal analysis.

EXPERIMENTAL

Synthesis of complex I. A mixture of aqueous solutions of $\text{K}_2[\text{PtCl}_4]$ (Merck) and $\text{K}\{\text{S}_2\text{P}(\text{O}-\text{iso}-\text{C}_4\text{H}_9)_2\}$ (Cheminova Agro A/S) was heated to 60°C and left overnight. The resulting yellow precipitate was filtered off, washed with water, and dried on the filter. An additional crop of the complex was gathered by extraction with chloroform. Complex **I** was recrystallized from chloroform to obtain single crystals for X-ray diffraction analysis.

Complex **I** and the starting reagent potassium O,O'-diisobutyl dithiophosphate (**II**) were characterized by ^{13}C MAS NMR spectroscopy:

Complex **I**, δ : (1 : 1 : 2) 74.6, 74.0 (1 : 1, $-\text{OCH}_2-$), 29.5, 29.3 (1 : 1, $-\text{CH}=\text{}$), 21.5, 20.7, 20.5, 19.9 ppm (1 : 1 : 1 : 1, $-\text{CH}_3$).

Compound **II**, δ : (1 : 1 : 2) 75.1, 74.2, 73.5, 73.2, 72.9 ($-\text{OCH}_2-$), 29.9, 29.8, 29.7 ($-\text{CH}=\text{}$), 21.1, 21.0, 20.9, 20.8, 20.7, 20.6, 20.4, 20.3, 20.2, 20.1 ppm ($-\text{CH}_3$).

^{13}C , ^{31}P , and ^{195}Pt CP/MAS NMR spectra were recorded on a CMX-360 spectrometer (Varian/Che-magnetics InfinityPlus) operating at 90.52, 145.72, and 76.99–77.22 MHz, respectively (superconducting magnet with $B_0 = 8.46$ T; Fourier transform). The ^1H – ^{13}C , ^1H – ^{31}P , and ^1H – ^{195}Pt cross polarization techniques were used; ^{13}C – ^1H , ^{31}P – ^1H , and ^{195}Pt – ^1H dipolar interactions were suppressed via proton decoupling in a magnetic field with the corresponding proton resonance frequency [6]. A sample (~350 mg) of complex **I** was packed into a zirconia rotor (7.5 mm in diameter). The spinning rates in $^{13}\text{C}/^{31}\text{P}$ MAS NMR experiments were 3600/2300–3800(1) Hz. The numbers of scans were 100/32, respectively. The proton $\pi/2$ -pulse durations were 6.0/7.0 μs . The ^1H – $^{13}\text{C}/^1\text{H}$ – ^{31}P contact times were 2.0/3.0 ms; the pulses were spaced at 3.0/3.0 s. Isotropic ^{13}C , ^{31}P , and ^{195}Pt chemical shifts δ (ppm) are referenced to a line of crystalline adamantane [7] used as the external standard (δ 38.48 ppm relative to tetramethylsilane [8]), 85% H_3PO_4 (0 ppm) [9], and 0.1 M $\text{H}_2[\text{PtCl}_6]$ (Merck) (0 ppm [10]; the corresponding ^{195}Pt resonance frequency is 77.3751 MHz), respectively.

In ^{195}Pt MAS NMR experiments, we used a direct excitation 90° -pulse (5.6 μs) to excite a spectral range of 45 kHz. ^{195}Pt – ^1H interactions were suppressed via proton decoupling in a magnetic field (amplitude $\gamma B_1/2\pi = 32.1$ kHz) with the corresponding proton resonance frequency (359.937 MHz). The phase modulation of the proton pulses was $\pm 15^\circ$ [11]. The total extent of the ^{195}Pt MAS NMR spectrum (~270 kHz) made it impossible to simultaneously excite the entire spectrum at a single carrier frequency. For this reason, we varied the carrier frequency with a step of 77 kHz to excite four regions of the spectrum at 76.991, 77.068, 77.145, and 77.222 MHz. The whole pattern was obtained by the summation of the spectra preceded by their shifting so that the central signal and all sidebands coincided. The spinning rate was 5000(1) Hz. For each region, the number of scans was 8556; the exciting pulses were spaced at 2.0 s. Since the initial region of the free induction decay (FID) diagram of the MAS NMR spectrum was distorted by the decay of the exciting pulse (due to the “ringdown” effect), the distorted range was cut off. To avoid phase distortions of the MAS NMR spectrum, the FID diagram was shifted (before Fourier transforms) toward the decay region by a required number of points. Since the FID diagram contained over 24 rotational echoes, the removal of the initial region did not

result in critical spectral changes. The magic angle was set at the ^{79}Br resonance frequency (90.183 MHz).

Additional adjustment was performed by minimizing the line widths in the ^{195}Pt MAS NMR spectrum of cooperite, which is characterized by a considerable anisotropy of the ^{195}Pt chemical shift ($\delta_{\text{aniso}} = 5873$ ppm, $\eta = 0.37$ [1, 2]) and by a high sensitivity of the line width to small deviations of the magic angle. The width of the reference line of adamantane (3.5 Hz) was used to check the homogeneity of the magnetic field. The δ_{iso} values were corrected for drift of the magnetic field strength (its frequency equivalents for the $^{13}\text{C}/^{31}\text{P}/^{195}\text{Pt}$ nuclei were 0.051/0.11/0.044 Hz/h). The chemical shifts and intensity ratios of the signals and the coupling constants were refined by fragment-by-fragment modeling of NMR spectra (Spinsight program) with regard to the line positions and widths and the contributions from the Lorentzian and Gaussian functions to the line shapes. The ^{31}P chemical shift anisotropy ($\delta_{\text{aniso}} = \delta_{zz} - \delta_{\text{iso}}$) and the asymmetry parameter ($\eta = (\delta_{yy} - \delta_{xx})/(\delta_{zz} - \delta_{\text{iso}})$) were calculated from diagrams of the χ^2 statistic [12]. Plotting of the diagrams was based on an analysis of the intensity ratios of the sidebands (due to spinning) [13] in the spectra recorded at two spinning rates. The calculations were performed with the Mathematica program (version 4.1.2) [14].

Single-crystal X-ray diffraction analysis of complex **I** was performed at 298(2) K on a BRUKER SMART 1000 CCD diffractometer (MoK_α radiation, $\lambda = 0.71073$ Å, graphite monochromator). Reflection intensities were measured in groups of 906 frames for $\varphi = 0^\circ, 90^\circ$, and 180° ; (ω scan mode, scan step 0.2° , frame exposure time 40 s). Absorption correction was applied from the face indices of the single crystal. Structure **I** was solved by the direct method and refined by the least-squares method in the anisotropic approximation for non-hydrogen atoms. The hydrogen atoms were located geometrically and refined in the riding model. The collected data were edited and the unit cell parameters were refined with the SMART and SAINT-Plus programs [15]. All calculations for structure determination and refinement were performed with the SHELXTL/PC programs [16].

Selected crystallographic parameters and a summary of data collection and refinement for structure **I** are given in Table 1. Bond lengths and angles are listed in Table 2. Atomic coordinates and other parameters of structure **I** have been deposited with the Cambridge Crystallographic Data Collection (no. 706517; deposit@ccdc.cam.ac.uk).

The thermal properties of complex I were studied by simultaneous recording of TG and DSC curves (combined thermal analysis). The study was carried out on a STA 449C Jupiter instrument (NETZSCH) in quartz crucibles. An opening in the caps of the crucibles provided a vapor pressure of 1 atm during thermolysis. A sample (4.43 mg) was heated under argon to 950°C at a heating rate of $5^\circ\text{C}/\text{min}$. The error in temperature

Table 1. Crystallographic parameters and a summary of data collection and refinement for structure **I**

Parameter	Value
Empirical formula	C ₁₆ H ₃₆ O ₄ P ₂ S ₄ Pt
<i>M</i>	677.74
Crystal system	Triclinic
Space group	<i>P</i> $\bar{1}$
<i>a</i> , Å	9.075(2)
<i>b</i> , Å	9.385(2)
<i>c</i> , Å	9.954(2)
α , deg	69.911(3)
β , deg	65.968(4)
γ , deg	65.877(3)
<i>V</i> , Å ³	690.5(2)
<i>Z</i>	1
ρ_{calcd} , g/cm ³	1.630
μ , mm ⁻¹	5.515
<i>F</i> (000)	336
Crystal shape (size, mm)	Prism (0.17 × 0.15 × 0.09)
θ scan range, deg	2.80–26.02
Ranges of <i>h</i> , <i>k</i> , and <i>l</i> indices	–11 ≤ <i>h</i> ≤ 11, –11 ≤ <i>k</i> ≤ 11, –12 ≤ <i>l</i> ≤ 12
Number of measured reflections	5252
Number of independent reflections	2650 (<i>R</i> _{int} = 0.0347)
Number of reflections with <i>I</i> > 2σ(<i>I</i>)	2629
Method of refinement	Full-matrix least-squares on <i>F</i> ²
Number of parameters refined	149
GOOF	1.022
R factors for <i>F</i> ² > 2σ(<i>F</i> ²)	<i>R</i> ₁ = 0.0348, <i>wR</i> ₂ = 0.0877
R factors for all reflections	<i>R</i> ₁ = 0.0351, <i>wR</i> ₂ = 0.0881
Residual electron density (min/max), e Å ⁻³	–0.572/1.805

measurements was ±1°C; the error in weight measurements was ±1 × 10⁻² mg.

RESULTS AND DISCUSSION

The ¹³C MAS NMR spectrum of complex **I** (Fig. 1a) shows signals for the –CH₂–, –CH=, and –CH₃ groups of the alkyl substituents in the Dtph ligands. Pairs of the ¹³C NMR signals for each group indicate their structural nonequivalence in adjacent chains of *iso*-C₄H₉. The presence of a single triplet (~1 : 4 : 1) in the centroid of the ³¹P MAS NMR spectrum (Fig. 1b) is indic-

ative of the structural equivalence of the Dtph fragments. Because naturally occurring platinum contains the ¹⁹⁵Pt nuclide (33.83 at%, $\mu = 0.60950 \mu_N$; *I* = 1/2), two symmetrically arranged satellite signals result from ³¹P and ¹⁹⁵Pt spin-spin couplings with the coupling constant ²*J*(³¹P–¹⁹⁵Pt) (Table 3).

The shapes of the ³¹P MAS NMR spectra suggest a nearly rhombic symmetry of the ³¹P chemical shift tensor. For quantitative estimation of the ³¹P chemical shift anisotropy, we plotted diagrams of the χ^2 statistic as a function of $\delta_{\text{aniso}} = (\delta_{zz} - \delta_{\text{iso}})$ and $\eta = (\delta_{zz} - \delta_{xx})/(\delta_{zz} - \delta_{\text{iso}})$. (At $\eta = 0$, the chemical shift tensor is axially symmetric. An increase in η from 0 to 1 reflects an increasing contribution from the rhombic component.) For complex **I**, $\eta = 0.73$ suggests a predominantly rhombic character of the ³¹P chemical shift tensor. According to $|\delta_{\text{aniso}}| = 38.1$ ppm (which correlates with the SPS angle [17–21]), this angle in complex **I** is expected to be greater than 101.8° found in [Pt{S₂P(O-*cyclo*-C₆H₁₁)₂}₂] [5] for $|\delta_{\text{aniso}}| = 30.8$ ppm (Table 3).

The shape of the whole ¹⁹⁵Pt MAS NMR spectrum of complex **I** (Fig. 1c) corresponds to the axially symmetric ¹⁹⁵Pt chemical shift tensor (for $\delta_{zz} > \delta_{xx}$ and δ_{yy} ; so $\delta_{\text{aniso}} > 0$). The character of the spectrum under discussion agrees with the concept of the formation of square chromophores [PtS₄] as in cooperite [1, 2]. The triplet structure (1 : 2 : 1) of the signal in the centroid of the ¹⁹⁵Pt MAS NMR spectrum (with the isotropic ¹⁹⁵Pt chemical shift) can be explained by spin-spin couplings between ¹⁹⁵Pt and ³¹P nuclei of two structurally equivalent Dtph ligands; the coupling constants ²*J*(¹⁹⁵Pt–³¹P) are given in Table 3.

To verify the conclusions drawn from the MAS NMR spectra, we determined structure **I** using X-ray diffraction analysis.

In centrosymmetric structure **I** (Fig. 2), the Pt atom coordinates two Dtph ligands in a S,S'-anisobidentate fashion (Pt–S 2.315 and 2.329 Å) to form the square chromophore [PtS₄] (*dsp*²-hybridization). The nonequivalence of the Pt–S bonds results in a slight rhombic distortion of the chromophore (S...S 90.34° and 89.66°). Another type of distortion is due to the fact that the S(1)–S(2) distance in the ligand (3.104 Å) is appreciably shorter than the S(1)–S(2)^a distance between the ligands (3.454 Å). The bidentate coordination of the Dtph ligands produces two four-membered chelate rings [PtS₂P] with platinum as a spiro atom. The torsion angles PtSSP (169.8°) and SPtPS (170.5°) deviate from 180° because of a tetrahedral distortion of the planar geometry of these rings. In the four-membered ring, the Pt...P distance is very short (2.964 Å).

As expected from ³¹P MAS NMR data, the SPS angle in structure **I** (102.39°) is greater than an analogous angle in [Pt{S₂P(O-*cyclo*-C₆H₁₁)₂}₂] [5] but almost exactly equals the corresponding value for [Pt{S₂P(OC₂H₅)₂}₂] [4]. On the whole, platinum(II) dialkyl dithiophosphates are characterized by the smallest values of this angle among similar complexes

Table 2. Selected bond lengths and angles in structure **I***

Bond	<i>d</i> , Å	Bond	<i>d</i> , Å
Pt–S(1)	2.329(1)	C(1)–C(2)	1.463(8)
Pt–S(2)	2.315(1)	C(2)–C(3)	1.520(1)
S(1)–P	1.997(2)	C(2)–C(4)	1.450(1)
S(2)–P	1.986(2)	C(5)–C(6)	1.450(1)
P–O(1)	1.564(4)	C(6)–C(7A)	1.440(1)
P–O(2)	1.566(4)	C(6)–C(7B)	1.430(1)
O(1)–C(1)	1.457(7)	C(6)–C(8A)	1.420(1)
O(2)–C(5)	1.458(9)	C(6)–C(8B)	1.440(1)
Angle	ω, deg	Angle	ω, deg
S(1)PtS(2)	83.89(5)	O(1)C(1)C(2)	110.1(4)
PS(1)Pt	86.13(5)	C(1)C(2)C(3)	108.9(5)
PS(2)Pt	86.75(5)	C(4)C(2)C(1)	113.9(6)
S(1)PS(2)	102.39(7)	C(4)C(2)C(3)	112.1(7)
O(1)PS(1)	114.8(2)	C(6)C(5)O(2)	110.3(6)
O(1)PS(2)	114.5(2)	C(8A)C(6)C(7A)	100.0(1)
O(2)PS(1)	114.7(2)	C(7B)C(6)C(8B)	120.0(1)
O(2)PS(2)	115.8(2)	C(8A)C(6)C(5)	111.9(9)
O(1)PO(2)	95.3(2)	C(7B)C(6)C(5)	113.0(9)
C(1)O(1)P	121.6(3)	C(7A)C(6)C(5)	121.0(1)
C(5)O(2)P	122.4(4)	C(8B)C(6)C(5)	113.0(1)

* The population of the positions C(7A) and C(8A) is 0.60; the population of the positions C(7B) and C(8B) is 0.40.

of other metals: nickel(II) -102.78° and 102.91° [22], zinc 109.11° and 115.73° [23, 24], cadmium 114.24° – 119.63° [18, 25–27], lead(II) 114.14° – 116.16° [17, 20, 28], silver(I) 116.22° – 117.6° [29], and antimony(V) 116.39° – 118.23° [21, 30, 31]. The sole exception is the isomers of $[\text{Ni}\{\text{S}_2\text{P}(\text{OC}_3\text{H}_7)_2\}_2]$ – 102.02° and 102.9° [22].

The P–S bond lengths (1.997 and 1.986 Å) in complex **I** are intermediate between the idealized values for the single and double phosphorus–sulfur bonds (2.14 and 1.94 Å, respectively) [32]. This is evidence for the delocalization of the π -electron density over the structural fragments PS_2 . The phosphorus atom is in the tetrahedral environment $[\text{O}_2\text{S}_2]$.

Despite a close structural similarity of the chromophores $[\text{PtS}_4]$ in complex **I** and cooperite, the Pt–S bonds in the latter are somewhat stronger and are equivalent (2.3108 and 2.3109 Å). In addition, all the angles SPtS in cooperite are 90° , while in structure **I**, the angle SPtS in the ligand is 83.89° and the angle SPtS between the ligands amounts to 96.11° because of the formation of sterically strained four-membered chelate rings. According to MAS NMR data, the ^{195}Pt chemical shift anisotropy for complex **I** (compared to cooperite) is less pronounced; this anisotropy is mainly contributed by the component δ_{zz} , which can be estimated from experimental spectra at -2100 ppm (for PtS, $\delta_{zz} = 4023$ ppm [1, 2]). The same factor is behind the difference between the isotropic ^{195}Pt chemical shifts. Clearly, the platinum nucleus in complex **I** is shielded in the direction perpendicular to the plane of the chromophore $[\text{PtS}_4]$ appreciably more strongly than in cooperite.

According to the TG curve (Fig. 3), the thermolysis of complex **I** involves several steps. Before the weight losses, the DSC curve shows an endothermic peak at 75.4°C . An independent of measurement revealed that this peak is due to the melting of the sample (extrapolation gave $\text{mp} = 72.4^\circ\text{C}$). The first thermolysis step covers a temperature range from 170 to 280°C . The main weight loss occurs in the steeply descending segment of the TG curve: the

Table 3. Parameters of the ^{31}P and ^{195}Pt MAS NMR spectra of crystalline dialkyl dithiophosphates with reference to 85% H_3PO_4 and 0.1 M $\text{H}_2[\text{PtCl}_6]$

Compound	^{31}P				^{195}Pt	
	δ_{iso} , ppm	$^2J(^{31}\text{P}-^{195}\text{Pt})$, Hz	δ_{aniso} , ppm*	η^*	δ_{iso} , ppm	$^2J(^{195}\text{Pt}-^{31}\text{P})$, Hz
$[\text{Pt}\{\text{S}_2\text{P}(\text{O-iso-C}_4\text{H}_9)_2\}_2]$ (I)	104.3	443.2 ± 0.5	-38.1 ± 0.1	0.73 ± 0.01	-4029.7	445 ± 5
$[\text{Pt}\{\text{S}_2\text{P}(\text{O-cyclo-C}_6\text{H}_{11})_2\}_2]$ [5]	99.0	433.2 ± 0.5	-30.8 ± 0.2	0.98 ± 0.02	-3963.6	435 ± 15
$\text{K}\{\text{S}_2\text{P}(\text{O-iso-C}_4\text{H}_9)_2\}$ (II) [19]	110.9		-123.0 ± 2.0	0.01 ± 0.14		

* $\delta_{\text{aniso}} = \delta_{zz} - \delta_{\text{iso}}$; $\eta = (\delta_{yy} - \delta_{xx})/(\delta_{zz} - \delta_{\text{iso}})$.

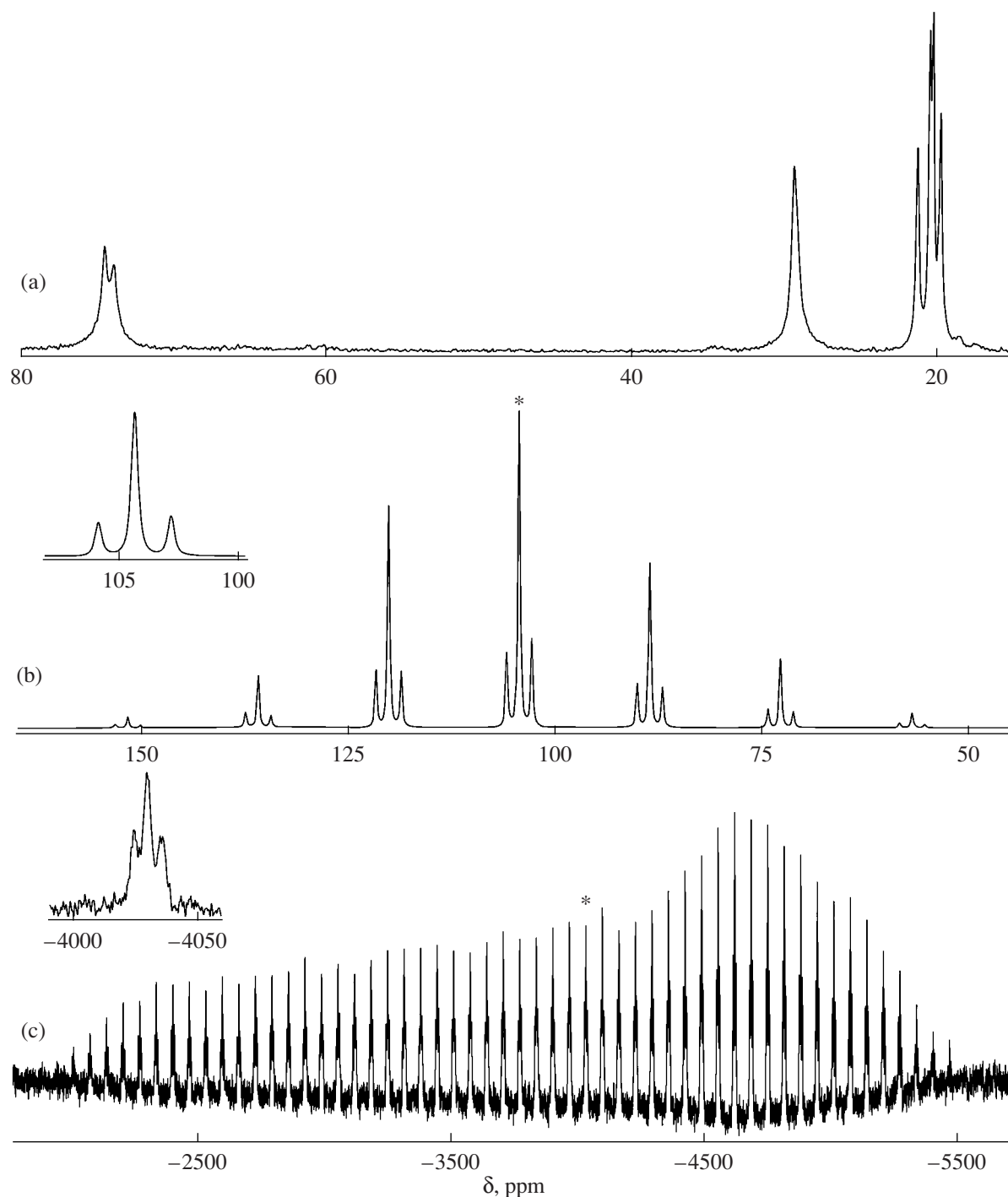


Fig. 1. (a) ^{13}C , (b) ^{31}P , and (c) ^{195}Pt MAS NMR spectra of $[\text{Pt}\{\text{S}_2\text{P}(\text{O-iso-C}_4\text{H}_9)_2\}_2]$ (**I**). The centroid signals in the spectra (b) and (c) are asterisked. The number of scans/spinning frequency (Hz) are (a) 100/3600, (b) 32/2300, and (c) 8556/5000.

DTG curve shows the maximum rate of the weight loss at 220.8°C . This weight loss (38.1%) is due to the formation of bis(dithiometaphosphato)platinum(II) ($[\text{Pt}(\text{S}_2\text{PO})_2]$, the calculated weight loss is 38.4%) as an intermediate product, which agrees with thermogravimetric data for liquid platinum(II)

dialkyl dithiophosphates [4]. The high-temperature range of the TG curve ($280\text{--}880^\circ\text{C}$) consists of four indistinct areas, thus suggesting a complicated character of the thermolysis of $[\text{Pt}(\text{S}_2\text{PO})_2]$. The weight of the final residue is 34.85% of the initial weight of the sample; according to [4], this corresponds to the

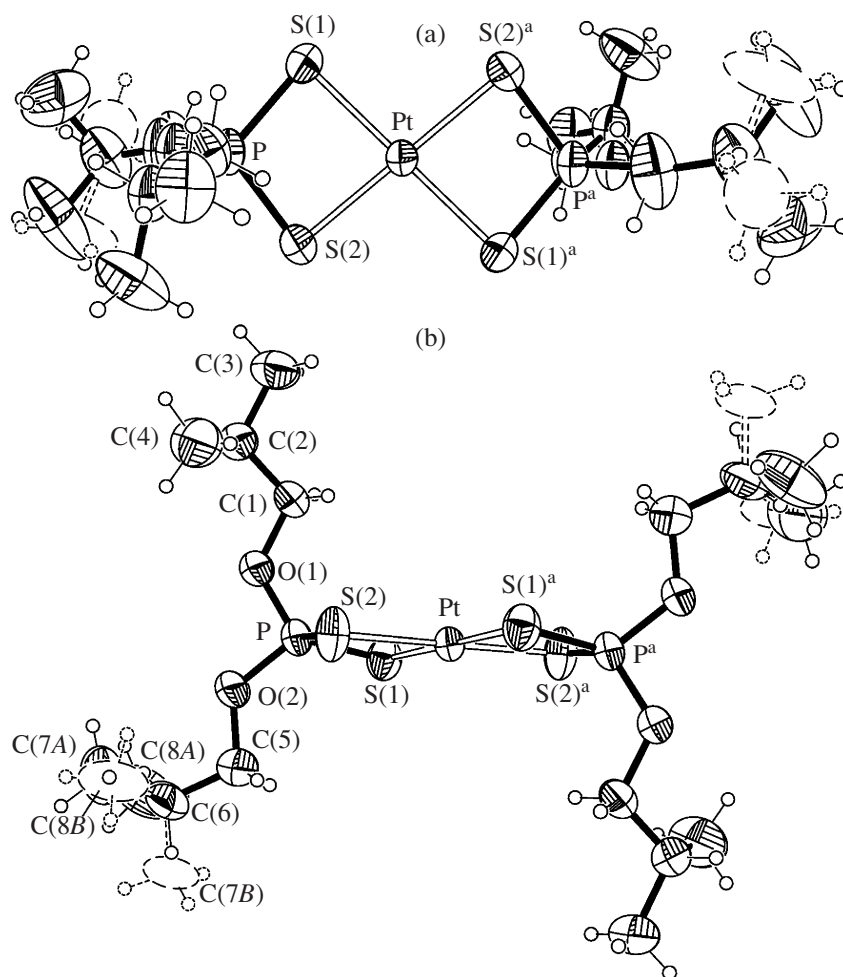


Fig. 2. Two projections of molecular structure **I** with atomic thermal displacement ellipsoids (50% probability).

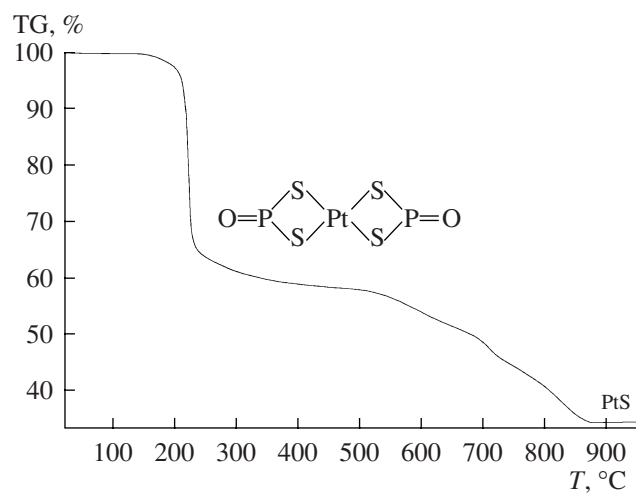


Fig. 3. TG curve of complex **I**.

formation of PtS contaminated with other thermolysis products (the calculated value is 33.50%).

ACKNOWLEDGMENTS

We are grateful to O.N. Antzutkin for his assistance in ^{195}Pt MAS NMR experiments and to Cheminova Agro A/S (Denmark) for providing potassium O,O'-diisobutyl dithiophosphate.

This work was supported by the Russian Foundation for Basic Research, project no. 08-03-00068-a.

REFERENCES

- Ivanov, A.V., Palazhchenko, V.I., Strikha, V.E., et al., *Dokl. Akad. Nauk*, 2006, vol. 410, no. 4, p. 512.
- Rozhdestvina, V.I., Ivanov, A.V., Zaremba, M.A., et al., *Kristallografiya*, 2008, vol. 53, no. 3, p. 428 [*Crystallogr. Rep.* (Engl. Transl.), vol. 53, no. 3, p. 391].
- Tkachev, V.V. and Atovmyan, L.O., *Koord. Khim.*, 1982, vol. 8, no. 2, p. 215.
- Gianini, M., Caseri, W.R., Gramlich, V., and Suter, U.W., *Inorg. Chim. Acta*, 2000, vol. 299, no. 2, p. 199.
- Ivanov, A.V., Lutsenko, I.A., Ivanov, M.A., et al., *Koord. Khim.*, 2008, vol. 34, no. 8, p. 591 [*Russ. J. Coord. Chem.* (Engl. Transl.), vol. 34, no. 18, p. 584].
- Pines, A., Gibby, M.G., and Waugh, J.S., *J. Chem. Phys.*, 1972, vol. 56, no. 4, p. 1776.
- Earl, W.L., VanderHart, D.L., *J. Magn. Reson.*, 1982, vol. 48, no. 1, p. 35.
- Morcombe, C.R. and Zilm, K.W., *J. Magn. Reson.*, 2003, vol. 162, no. 2, p. 479.
- Karaghiosoff, K., *Encyclopedia of Nuclear Magnetic Resonance*, Grant, D.M. and Harris, R.K., Eds., New York: Wiley, 1996, vol. 6, p. 3612.
- Kirakosyan, G.A., *Koord. Khim.*, 1993, vol. 19, no. 7, p. 507.
- Bennett, A.E., Rienstra, Ch.M., Auger, M., et al., *J. Chem. Phys.*, 1995, vol. 103, no. 16, p. 6951.
- Press, W.H., Teukolsky, S.A., Vetterling, W.T., and Flannery, B.P., *Numerical Recipes in C*, Cambridge: Cambridge Univ., 1994.
- Hodgkinson, P. and Emsley, L., *J. Chem. Phys.*, 1997, vol. 107, no. 13, p. 4808.
- Wolfram, S., *The Mathematica Book*, Cambridge: Wolfram Media / Cambridge Univ., 1999.
- SMART and SAINT-Plus. Version 5.0. Data Collection and Processing Software for the SMART System*, Madison (WI, USA): Bruker AXS, 1998.
- SHELXTL/PC. Version 5.10. An Integrated System for Solving, Refining and Displaying Crystal Structures from Diffraction Data*, Madison (WI, USA): Bruker AXS, 1998.
- Larsson, A.-C., Ivanov, A.V., Antzutkin, O.N., et al., *Inorg. Chim. Acta*, 2004, vol. 357, no. 9, p. 2510.
- Ivanov, A.V., Gerasimenko, A.V., Antzutkin, O.N., and Forsling, W., *Inorg. Chim. Acta*, 2005, vol. 358, no. 9, p. 2585.
- Larsson, A.-C., Ivanov, A.V., Forsling, W., et al., *J. Am. Chem. Soc.*, 2005, vol. 127, no. 7, p. 2218.
- Larsson, A.-C., Ivanov, A.V., Pike, K.J., et al., *J. Magn. Reson.*, 2005, vol. 177, no. 1, p. 56.
- Ivanov, M.A., Antzutkin, O.N., Sharutin, V.V., et al., *Inorg. Chim. Acta*, 2007, vol. 360, no. 9, p. 2897.
- Ivanov, A.V., Larsson, A.-C., Rodionova, N.A., et al., *Zh. Neorg. Khim.*, 2004, vol. 49, no. 3, p. 423 [*Russ. J. Inorg. Chem.* (Engl. Transl.), vol. 49, no. 3, p. 373].
- Ivanov, A.V., Forsling, W., Kritikos, M., et al., *Dokl. Chem.*, 2000, vol. 375, nos. 1–3, p. 195 [*Dokl.* (Engl. Transl.), vol. 375, no. 2, p. 236].
- Ivanov, A.V., Antzutkin, O.N., Larsson, A.-C., et al., *Inorg. Chim. Acta*, 2001, vol. 315, no. 1, p. 26.
- Ivanov, A.V., Antzutkin, O.N., Forsling, W., et al., *Dokl. Chem.*, 2002, vol. 387, nos. 4–6, p. 500 [*Dokl.* (Engl. Transl.), vol. 387, no. 4, p. 299].
- Ivanov, A.V., Antzutkin, O.N., Forsling, W., and Rodionova, N.A., *Koord. Khim.*, 2003, vol. 29, no. 5, p. 766 [*Russ. J. Coord. Chem.* (Engl. Transl.), vol. 29, no. 5, p. 714].
- Yin, Y.-G., Forsling, W., Bostrom, D., et al., *Chin. J. Chem.*, 2003, vol. 21, no. 3, p. 291.
- Larsson, A.-C., Ivanov, A.V., Antzutkin, O.N., and Forsling, W., *J. Colloid Interface Sci.*, 2008, vol. 327, no. 2, p. 370.
- Ivanov, A.V., Zinkin, S.A., Gerasimenko, A.V., et al., *Koord. Khim.*, 2007, vol. 33, no. 1, p. 22 [*Russ. J. Coord. Chem.* (Engl. Transl.), vol. 33, no. 1, p. 20].
- Ivanov, M.A., Sharutin, V.V., Ivanov, A.V., et al., *Koord. Khim.*, 2008, vol. 34, no. 7, p. 533 [*Russ. J. Coord. Chem.* (Engl. Transl.), vol. 34, no. 7, p. 527].
- Ivanov, M.A., Sharutin, V.V., Ivanov, A.V., et al., *Zh. Neorg. Khim.*, 2009, vol. 54, no. 5.
- Lawton, S.L. and Kokotailo, G.T., *Inorg. Chem.*, 1969, vol. 8, no. 11, p. 2410.